

Variational asymptotic method for unit cell homogenization of periodically heterogeneous materials [☆]

Wenbin Yu ^{*}, Tian Tang

Department of Mechanical and Aerospace Engineering, Utah State University, Logan, UT 80322-4130, USA

Received 9 January 2006; received in revised form 4 October 2006

Available online 21 October 2006

Abstract

A new micromechanics model, namely, the variational asymptotic method for unit cell homogenization (VAMUCH), is developed to predict the effective properties of periodically heterogeneous materials and recover the local fields. Considering the periodicity as a small parameter, we can formulate a variational statement of the unit cell through an asymptotic expansion of the energy functional. It is shown that the governing differential equations and periodic boundary conditions of mathematical homogenization theories (MHT) can be reproduced from this variational statement. In comparison to other approaches, VAMUCH does not rely on ad hoc assumptions, has the same rigor as MHT, has a straightforward numerical implementation, and can calculate *the complete set of properties simultaneously without using multiple loadings*. This theory is implemented using the finite element method and an engineering program, VAMUCH, is developed for micromechanical analysis of unit cells. Many examples of binary composites, fiber reinforced composites, and particle reinforced composites are used to demonstrate the application, power, and accuracy of the theory and the code of VAMUCH. © 2006 Elsevier Ltd. All rights reserved.

Keywords: Homogenization; Unit cell; Heterogeneous; Anisotropic; Variational asymptotic method; VAMUCH

1. Introduction

Along with the increased knowledge and fabrication techniques for materials, more and more structures are made with heterogeneous materials with engineered microstructures to achieve the ever-increasing performance requirements. The increased complexity at the microlevel greatly complicates the analysis of the structural behavior, which is indispensable for rational designs of these structures. Although it is logically sound to use the well-established finite element method (FEM) to analyze such structures by meshing all the details of constituent materials, the size of the finite element model will easily overpower most of the computers we can

[☆] Parts of this paper appeared in the proceedings of 2005 ASME International Mechanical Engineering Congress and Exposition, Orlando, Florida, Nov. 5–11, 2005 and the 47th Structures, Structural Dynamics, and Materials Conference, Newport, Rhode Island, May 1–4, 2006.

^{*} Corresponding author. Tel.: +1 435 7978246; fax: +1 435 7972417.

E-mail address: wenbin.yu@usu.edu (W. Yu).

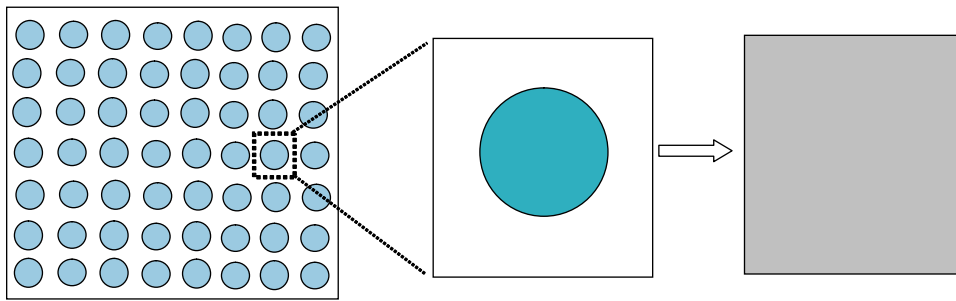


Fig. 1. Periodic heterogeneous materials and the corresponding unit cell.

access in the foreseeable future because the macroscopic structural dimensions are usually several orders of magnitude larger than the characteristic size of constituent materials.

If the structure can be idealized as a periodic assembly of *many* unit cells (UCs, see Fig. 1), it is possible to homogenize the heterogeneous UC with a set of effective material properties obtained by a micromechanical analysis of the UC. As illustrated in Fig. 2, the concept of UC essentially simplifies the original expensive analysis of structures made with heterogeneous materials using the following three steps:

- Identify the UC and carry out a micromechanical analysis of the UC to obtain effective material properties;
- Analyze the structure with homogenized material properties to study the macroscopic structural behavior;
- Feedback the macroscopic behavior to the micromechanical analysis to calculate local fields such as displacements, strains, and stresses within the UC, which are only needed for detailed analysis of some critical zones.

In the past several decades, numerous approaches have been proposed for the micromechanical analysis of UCs (see Hashin (1983) and references cited therein). These includes the earliest rules of mixture approaches based on Voigt and Reuss hypotheses. Hill (1952) has shown that Voigt and Reuss assumptions predict the upper and lower bounds, respectively, for the effective elastic properties of the homogenized UC. For general heterogeneous materials, the difference between these two bounds could be too large to be of practical use.

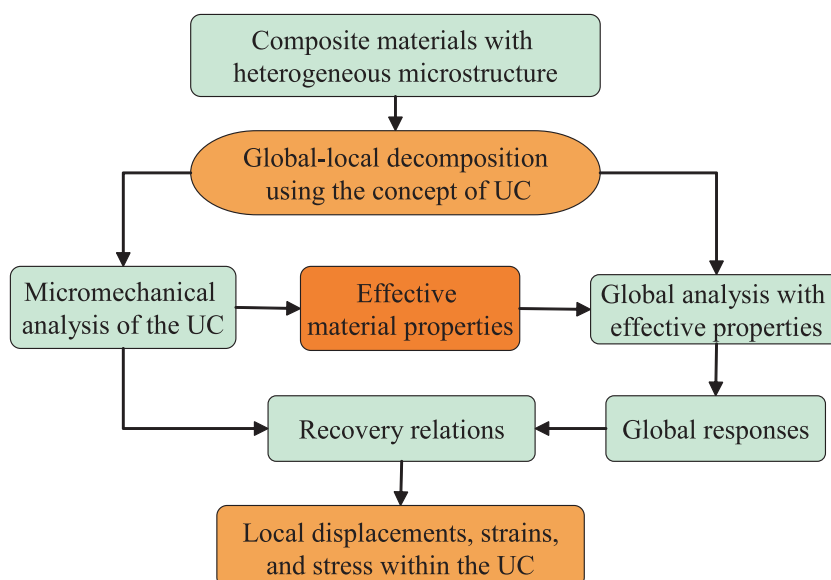


Fig. 2. The basic steps of structure analysis with heterogeneous microstructures using the concept of unit cell.

Researchers have proposed various techniques to either reduce the difference between the upper and lower bounds, or find an approximate value between the upper and lower bounds. Typical approaches are the self-consistent model (Hill, 1965) and its generalizations (Dvorak and Bahei-El-Din, 1979; Accorsi and Nemat-Nasser, 1986), the variational approach of Hashin and Shtrikman (1962), third-order bounds (Milton, 1981), the method of cells (MOC) (Aboudi, 1982, 1989) and its variants (Paley and Aboudi, 1992; Aboudi et al., 2001; Williams, 2005b), recursive cell method (Banerjee and Adams, 2004), mathematical homogenization theories (MHT) (Bensoussan et al., 1978; Murakami and Toledano, 1990), finite element approaches using conventional stress analysis of a representative volume element (RVE) (Sun and Vaidya, 1996), and many others. Hollister and Kikuchi (1992) compared different approaches and concluded that MHT is preferable over other approaches for periodic composites even when the material is only locally periodic with a finite periodicity. Although MOC is not compared in Hollister and Kikuchi (1992), MOC expands the local displacements in terms of global displacements using the Legendre polynomial of different orders according to the required accuracy. The accuracy of MOC could be comparable to MHT if sufficient terms are used in the polynomial expansion although the asymptotical correctness cannot be guaranteed. It is interesting to notice that the author of MOC recently developed a new micromechanical analysis (Aboudi et al., 2001) based on MHT with the solution procedure borrowed from MOC.

Although different approaches adopt different assumptions in the literature, there are only two essential assumptions associated with the micromechanical analysis of heterogeneous materials with identifiable UCs.

Assumption 1. The exact solutions of the field variables have volume averages over the UC. For example, if u_i are the exact displacements within the UC, there exist v_i such that

$$v_i = \frac{1}{\Omega} \int_{\Omega} u_i d\Omega \equiv \langle u_i \rangle \quad (1)$$

where Ω denotes the domain occupied by the UC and its volume.

Assumption 2. The effective material properties obtained from the micromechanical analysis of the UC are independent of the geometry, the boundary conditions, and loading conditions of the macroscopic structure, which means that effective material properties are assumed to be the intrinsic properties of the material when viewed macroscopically.

Of course, the micromechanical analysis of the UC is only needed and appropriate if $\eta = h/l \ll 1$, with h as the characteristic size of the UC and l as the characteristic wavelength of the deformation of the structure. *All the others assumptions such as particular geometry shape and arrangement of the constituents, specific boundary conditions, and prescribed relations between local fields and global fields are convenient but not essential.*

In this study, the variational asymptotic method (VAM) of Berdichevsky (1979) will be used to develop a new unit cell homogenization technique invoking these two essential assumptions. VAM simplifies the procedure of solving physical problems that can be formulated in terms of a variational statement involving one or more small parameters. In contrast to conventional asymptotic methods, VAM carries out asymptotic analysis of the variational statement, synthesizing both merits of variational methods (viz., systematic, simple, and easy to be implemented numerically) and asymptotic methods (viz., without *ad hoc* assumptions). VAM has been used extensively to construct efficient high-fidelity structure models for composite beams (Yu et al., 2002c), composite and smart plates (Yu et al., 2002a; Yu and Hodges, 2004a,b), and composite and smart shells (Yu et al., 2002b, 2005), achieving an excellent compromise between accuracy and efficiency. VAM has also been used to homogenize isotropic material with periodic cavities (Berdichevsky, 1977), which laid a foundation for the present work.

First, we extend the work of Berdichevsky (1977) to extract a variational statement for the micromechanical analysis of the UC from the three-dimensional (3D) continuum formulation of the periodically heterogeneous, anisotropic materials. This variational statement can be solved using VAM asymptotically to find the relation between the local displacements and global displacements for the purpose to predict effective material properties and local fields. Then we will implement this theory using FEM to develop an engineering code, VAMUCH, to uniformly handle general heterogeneous microstructures including one-dimensional (1D),

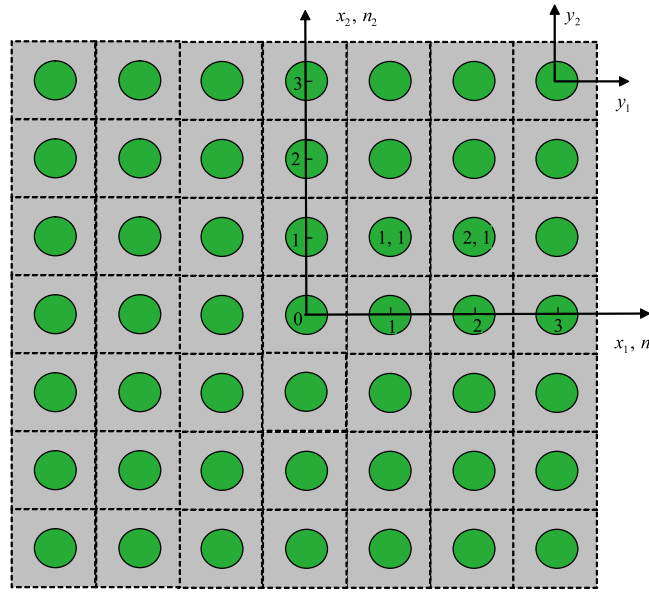


Fig. 3. Coordinate systems for 2D heterogeneous materials.

two-dimensional (2D), or 3D UCs. Finally, many examples including binary composites, fiber reinforced composites, and particle reinforced composites, are used to demonstrate the application, power, and accuracy of the present theory and the companion code VAMUCH.

2. A variational statement for unit cells

As shown in Fig. 3, to facilitate our formulation, we need to setup three coordinate systems: two cartesian coordinates $\mathbf{x} = (x_1, x_2, x_3)$ and $\mathbf{y} = (y_1, y_2, y_3)$, and an integer-valued coordinate $\mathbf{n} = (n_1, n_2, n_3)$. We use x_i as the global coordinates to describe the macroscopic structure and y_i parallel to x_i as the local coordinates to describe the UC (Here and throughout the paper, Latin indices assume 1, 2, and 3 and repeated indices are summed over their range except where explicitly indicated). If the UC is a cube with dimensions as d_i , we chose the local coordinates y_i in such a way that $y_i \in [-d_i/2, d_i/2]$. Since the heterogeneous material composes of many countable UCs, it is also convenient to introduce integer coordinates n_i to locate each individual UC. The integer coordinates are related to the global coordinates in such a way that $n_i = x_i/d_i$ (no summation over i). If the material is uniform in one of the directions, such as the fiber reinforced composites in the fiber direction, the dimension of that direction can be chosen to be an arbitrary length different from zero.

To formulate a variational statement for UCs, we need to use one of the energy principles, such as the principle of minimum total potential energy. The second assumption implies that we could obtain the same effective material properties from an imaginary unbounded and unloaded heterogeneous material with the same microstructure as the loaded and bounded one. Hence we could derive the micromechanical analysis from a heterogeneous material which could completely occupy the 3D space \mathcal{R} and composes of infinite many UCs. For elastic material,¹ the total potential energy is equal to the summation of the strain energy stored in all the UCs, which is:

$$\Pi = \sum_{n=-\infty}^{\infty} \int_{\Omega} \frac{1}{2} C_{ijkl}(y_1, y_2, y_3) \epsilon_{ij} \epsilon_{kl} d\Omega \quad (2)$$

¹ Although it is possible to use the present methodology to obtain inelastic properties of heterogeneous materials, we will focus on elastic properties in this study.

where C_{ijkl} are the components of the periodically varying fourth-order elasticity tensor and ϵ_{ij} are the components of the 3D strain tensor defined for linear theory as

$$\epsilon_{ij}(\mathbf{n}; \mathbf{y}) = \frac{1}{2} \left[\frac{\partial u_i(\mathbf{n}; \mathbf{y})}{\partial y_j} + \frac{\partial u_j(\mathbf{n}; \mathbf{y})}{\partial y_i} \right] \quad (3)$$

Here $u_i(\mathbf{n}; \mathbf{y})$ are functions of the integer coordinates and the local coordinates for each UC. In view of the fact that the infinite many UCs form a continuous heterogeneous material, we need to enforce the continuity of the displacement field u_i on the interface between adjacent UCs, which can be written as follows for a UC with integer coordinates (n_1, n_2, n_3) :

$$\begin{aligned} u_i(n_1, n_2, n_3; d_1/2, y_2, y_3) &= u_i(n_1 + 1, n_2, n_3; -d_1/2, y_2, y_3) \\ u_i(n_1, n_2, n_3; y_1, d_2/2, y_3) &= u_i(n_1, n_2 + 1, n_3; y_1, -d_2/2, y_3) \\ u_i(n_1, n_2, n_3; y_1, y_2, d_3/2) &= u_i(n_1, n_2, n_3 + 1; y_1, y_2, -d_3/2) \end{aligned} \quad (4)$$

According to the principle of minimum total potential energy, the exact solution will minimize the energy in Eq. (2) under the constraints in Eqs. (1) and (4). Although correctly formulated, this problem is very difficult to solve due to discrete integer arguments. To take advantage of well-developed analytical techniques for continuous functions, we need to transform the formulation into a more convenient format using the idea of quas-continuum (Kunin, 1982). The basic idea is to associate a function of integer arguments defined in the integer space with a continuous function defined in \mathcal{R} . Following the procedures spelled out in Berdichevsky (1977), we can reformulate Eqs. (2)–(4), respectively, as:

$$\Pi = \int_{\mathcal{R}} \left\langle \frac{1}{2} C_{ijkl} \epsilon_{ij} \epsilon_{kl} \right\rangle d\mathcal{R} \quad (5)$$

$$\epsilon_{ij}(\mathbf{x}; \mathbf{y}) = \frac{1}{2} \left[\frac{\partial u_i(\mathbf{x}; \mathbf{y})}{\partial y_j} + \frac{\partial u_j(\mathbf{x}; \mathbf{y})}{\partial y_i} \right] \equiv u_{(ij)} \quad (6)$$

and

$$\begin{aligned} u_i(x_1, x_2, x_3; d_1/2, y_2, y_3) &= u_i(x_1 + d_1, x_2, x_3; -d_1/2, y_2, y_3) \\ u_i(x_1, x_2, x_3; y_1, d_2/2, y_3) &= u_i(x_1, x_2 + d_2, x_3; y_1, -d_2/2, y_3) \\ u_i(x_1, x_2, x_3; y_1, y_2, d_3/2) &= u_i(x_1, x_2, x_3 + d_3; y_1, y_2, -d_3/2) \end{aligned} \quad (7)$$

Using the technique of Lagrange multipliers, we can pose the variational statement of the micromechanical analysis of UC as a stationary value problem of the following functional:

$$\begin{aligned} J &= \frac{1}{2} \int_{\mathcal{R}} [\langle C_{ijkl} u_{(ij)} u_{(kl)} \rangle + \lambda_i (\langle u_i \rangle - v_i)] d\mathcal{R} \\ &+ \int_{\mathcal{R}} \int_{S_1} \beta_{i1} [u_i(x_1, x_2, x_3; d_1/2, y_2, y_3) - u_i(x_1 + d_1, x_2, x_3; -d_1/2, y_2, y_3)] dS_1 d\mathcal{R} \\ &+ \int_{\mathcal{R}} \int_{S_2} \beta_{i2} [u_i(x_1, x_2, x_3; y_1, d_2/2, y_3) - u_i(x_1, x_2 + d_2, x_3; y_1, -d_2/2, y_3)] dS_2 d\mathcal{R} \\ &+ \int_{\mathcal{R}} \int_{S_3} \beta_{i3} [u_i(x_1, x_2, x_3; y_1, y_2, d_3/2) - u_i(x_1, x_2, x_3 + d_3; y_1, y_2, -d_3/2)] dS_3 d\mathcal{R} \end{aligned} \quad (8)$$

where λ_i and β_{ij} are Lagrange multipliers introducing constraints in Eqs. (1) and (7), respectively, and S_i are the surfaces with $n_i = 1$. Because v_i is unvarying for the UC, our problem is to find the displacement field u_i vanishing the first variation of J , which is solved asymptotically using VAM in the following section.

3. Variational asymptotic method for unit cell homogenization

In view of Eq. (1), it is natural to express the exact solution u_i as a sum of the volume average v_i plus the difference, such that

$$u_i(\mathbf{x}; \mathbf{y}) = v_i(\mathbf{x}) + w_i(\mathbf{x}; \mathbf{y}) \quad (9)$$

where $\langle w_i \rangle = 0$ according to Eq. (1). The very reason that the heterogeneous material can be homogenized leads us to believe that w_i should be asymptotically smaller than v_i , i.e.,

$$w_i \sim \eta v_i \quad (10)$$

Substituting Eq. (9) into Eq. (8) and making use of Eqs. (6) and (10), we can obtain the leading terms of the functional as:

$$\begin{aligned} J_1 = & \frac{1}{2} \int_{\mathcal{R}} [\langle C_{ijkl} w_{(i|j)} w_{(k|l)} \rangle + \lambda_i \langle w_i \rangle] d\mathcal{R} \\ & + \int_{\mathcal{R}} \int_{S_1} \beta_{i1} \left[w_i(\mathbf{x}; d_1/2, y_2, y_3) - w_i(\mathbf{x}; -d_1/2, y_2, y_3) - \frac{\partial v_i}{\partial x_1} d_1 \right] dS_1 d\mathcal{R} \\ & + \int_{\mathcal{R}} \int_{S_2} \beta_{i2} \left[w_i(\mathbf{x}; y_1, d_2/2, y_3) - w_i(\mathbf{x}; y_1, -d_2/2, y_3) - \frac{\partial v_i}{\partial x_2} d_2 \right] dS_2 d\mathcal{R} \\ & + \int_{\mathcal{R}} \int_{S_3} \beta_{i3} \left[w_i(\mathbf{x}; y_1, y_2, d_3/2) - w_i(\mathbf{x}; y_1, y_2, -d_3/2) - \frac{\partial v_i}{\partial x_3} d_3 \right] dS_3 d\mathcal{R}. \end{aligned} \quad (11)$$

Although it is possible to carry out the variation of J_1 and find the Euler-Lagrange equations and associated boundary conditions for w_i , which corresponds to homogenous governing differential equations along with inhomogeneous boundary conditions. It is more convenient to use change of variables to reformulate the same problem so that inhomogeneous governing differential equations along with homogeneous boundary conditions can be obtained. Considering the last three terms in Eq. (11), we use the following change of variables:

$$w_i(\mathbf{x}; \mathbf{y}) = y_j \frac{\partial v_i}{\partial x_j} + \chi_i(\mathbf{x}; \mathbf{y}) \quad (12)$$

with χ termed as fluctuation functions. Notice, we still have $\langle \chi_i \rangle = 0$ if the origin of the local system is chosen to be the center of UC. Then from the functional J_1 in Eq. (11), we can obtain the following functional defined over a UC:

$$\begin{aligned} J_1^* = & \frac{1}{2} \langle C_{ijkl} [\bar{\epsilon}_{ij} + \chi_{(i|j)}] [\bar{\epsilon}_{kl} + \chi_{(k|l)}] \rangle + \lambda_i \langle \chi_i \rangle \\ & + \int_{S_1} \beta_{i1} [\chi_i(\mathbf{x}; d_1/2, y_2, y_3) - \chi_i(\mathbf{x}; -d_1/2, y_2, y_3)] dS_1 + \int_{S_2} \beta_{i2} [\chi_i(\mathbf{x}; y_1, d_2/2, y_3) - \chi_i(\mathbf{x}; y_1, -d_2/2, y_3)] dS_2 \\ & + \int_{S_3} \beta_{i3} [\chi_i(\mathbf{x}; y_1, y_2, d_3/2) - \chi_i(\mathbf{x}; y_1, y_2, -d_3/2)] dS_3 \end{aligned} \quad (13)$$

where $\bar{\epsilon}_{ij} = v_{(i,j)}$ will be shown later to be the components of the global strain tensor for the structure with homogenized effective material properties. The functional J_1^* in Eq. (13) forms the backbone of the present theory, variational asymptotic method for unit cell homogenization (VAMUCH). Performing the variation, we can obtain conditions for J_1^* to be stationary as:

$$\frac{\partial}{\partial y_l} C_{ijkl} (\bar{\epsilon}_{ij} + \chi_{(i|j)}) = 0 \quad \text{in } \Omega \quad (14)$$

$$\chi_i(\mathbf{x}; d_1/2, y_2, y_3) = \chi_i(\mathbf{x}; -d_1/2, y_2, y_3) \quad (15)$$

$$\chi_i(\mathbf{x}; y_1, d_2/2, y_3) = \chi_i(\mathbf{x}; y_1, -d_2/2, y_3) \quad (16)$$

$$\chi_i(\mathbf{x}; y_1, y_2, d_3/2) = \chi_i(\mathbf{x}; y_1, y_2, -d_3/2) \quad (17)$$

$$C_{ijkl}(\bar{\epsilon}_{ij} + \chi_{(i|j)})|_{y_1=d_1/2} = C_{ijkl}(\bar{\epsilon}_{ij} + \chi_{(i|j)})|_{y_1=-d_1/2} \quad (18)$$

$$C_{ijkl}(\bar{\epsilon}_{ij} + \chi_{(i|j)})|_{y_2=d_2/2} = C_{ijkl}(\bar{\epsilon}_{ij} + \chi_{(i|j)})|_{y_2=-d_2/2} \quad (19)$$

$$C_{ijkl}(\bar{\epsilon}_{ij} + \chi_{(i|j)})|_{y_3=d_3/2} = C_{ijkl}(\bar{\epsilon}_{ij} + \chi_{(i|j)})|_{y_3=-d_3/2} \quad (20)$$

$$\langle \chi_i \rangle = 0 \quad (21)$$

where Eq. (14) is the governing differential equations, Eqs. (15)–(17) are the periodic boundary conditions for fluctuation functions, and Eqs. (18)–(20) are the periodic boundary conditions for local stresses. All these equations are identical to those of MHT, as listed in Manevitch et al. (2002). Although VAMUCH can reproduce the results of MHT as expected, VAMUCH is different from MHT in the following aspects:

- The periodic boundary conditions are derived in VAMUCH, while they are assumed *a priori* in MHT.
- The fluctuation functions are determined uniquely in VAMUCH due to Eq. (21), while they can only be determined up to a constant in MHT.
- VAMUCH has an inherent variational nature which is convenient for numerical implementation, while virtual quantities should be carefully chosen to make MHT variational as shown in Guedes and Kikuchi (1990).

The difficulty of solving the variational problem in Eq. (13) is tantamount to 3D anisotropic elasticity problems. Closed-form solutions exist only for very simple cases. For general cases we need to turn to numerical techniques such as FEM for approximate solutions.

4. Finite element implementation of VAMUCH

It is possible to formulate the FEM solution based on Eq. (13), however, it is not the most convenient and efficient way. First, Lagrange multipliers will increase the number of unknowns. Second, the linear system will have zeros on the diagonal of the coefficient matrix eluding the use of common LU decomposition technique. Considering the problem governed by Eqs. (14)–(21), the last equation, Eq. (21), will not affect the solution obtained by the rest of equations, which means the variational statement in Eq. (13) can be reformulated as seeking the minimum value of the following functional Π_Ω

$$\Pi_\Omega = \frac{1}{2\Omega} \int_\Omega C_{ijkl}[\bar{\epsilon}_{ij} + \chi_{(i|j)}][\bar{\epsilon}_{kl} + \chi_{(k|l)}] d\Omega \quad (22)$$

under the constraints in Eqs. (15)–(17). The constraints in Eq. (21) do not affect the minimum value of Π_Ω but help uniquely determine χ_i . In practice, we can constrain the fluctuation functions at an arbitrary node to be zero and later use these constraints to recover the unique fluctuation functions. It is fine to use penalty function method to introduce the periodic boundary conditions in Eqs. (15)–(17), as shown in Hollister and Kikuchi (1992). However, this method introduces additional approximation and the robustness of the solution depends on the choice of large penalty number. Here, we choose to make the nodes on the positive boundary surface (i.e., $y_i = d_i/2$) slave to the nodes on the opposite negative boundary surface (i.e., $y_i = -d_i/2$). By assembling all the independent active degrees of freedom, we can implicitly and exactly incorporate the periodic boundary conditions in Eqs. (15)–(17). In this way, we also reduce the total number of unknowns in the linear system.

Introduce the following matrix notations

$$\bar{\epsilon} = [\bar{\epsilon}_{11} \ 2\bar{\epsilon}_{12} \ \bar{\epsilon}_{22} \ 2\bar{\epsilon}_{13} \ 2\bar{\epsilon}_{23} \ \bar{\epsilon}_{33}]^T \quad (23)$$

$$\begin{Bmatrix} \frac{\partial \chi_1}{\partial y_1} \\ \frac{\partial \chi_1}{\partial y_2} + \frac{\partial \chi_2}{\partial y_1} \\ \frac{\partial \chi_2}{\partial y_2} \\ \frac{\partial \chi_1}{\partial y_3} + \frac{\partial \chi_3}{\partial y_1} \\ \frac{\partial \chi_2}{\partial y_3} + \frac{\partial \chi_3}{\partial y_2} \\ \frac{\partial \chi_3}{\partial y_3} \end{Bmatrix} = \begin{bmatrix} \frac{\partial}{\partial y_1} & 0 & 0 \\ \frac{\partial}{\partial y_2} & \frac{\partial}{\partial y_1} & 0 \\ 0 & \frac{\partial}{\partial y_2} & 0 \\ \frac{\partial}{\partial y_3} & 0 & \frac{\partial}{\partial y_1} \\ 0 & \frac{\partial}{\partial y_3} & \frac{\partial}{\partial y_2} \\ 0 & 0 & \frac{\partial}{\partial y_3} \end{bmatrix} \begin{Bmatrix} \chi_1 \\ \chi_2 \\ \chi_3 \end{Bmatrix} \equiv \Gamma_h \chi \quad (24)$$

where Γ_h is an operator matrix and χ is a column matrix containing the three components of the fluctuation functions. If we discretize χ using the finite elements as

$$\chi(x_i; y_i) = S(y_i) \mathcal{X}(x_i) \quad (25)$$

where S representing the shape functions (in the assembled sense disregarding the constrained node and slave nodes) and \mathcal{X} a column matrix of the nodal values of the fluctuation functions for all active nodes. Substituting Eqs. (23)–(25) into Eq. (22), we obtain a discretized version of the functional as

$$\Pi_\Omega = \frac{1}{2\Omega} (\mathcal{X}^T E \mathcal{X} + 2\mathcal{X}^T D_{he} \bar{\epsilon} + \bar{\epsilon}^T D_{ee} \bar{\epsilon}) \quad (26)$$

where

$$E = \int_\Omega (\Gamma_h S)^T D (\Gamma_h S) d\Omega \quad D_{he} = \int_\Omega (\Gamma_h S)^T D d\Omega \quad D_{ee} = \int_\Omega D d\Omega \quad (27)$$

with D as the 6×6 material matrix condensed from the fourth-order elasticity tensor C_{ijkl} . Since the periodic constraints have already been incorporated through assembly in Eq. (25), our problem becomes to minimize Π_Ω in Eq. (26), which gives us the following linear system

$$E \mathcal{X} = -D_{he} \bar{\epsilon} \quad (28)$$

It is clear that \mathcal{X} will linearly depend on $\bar{\epsilon}$, which means it is unnecessary to assign values to $\bar{\epsilon}$ (even 1's and 0's as in common practice), and they can be treated as symbols without entering the computation. The solution can be written as

$$\mathcal{X} = \mathcal{X}_0 \bar{\epsilon} \quad (29)$$

Substituting Eq. (29) into Eq. (26), we can calculate the energy storing in the UC

$$\Pi_\Omega = \frac{1}{2\Omega} \bar{\epsilon}^T (\mathcal{X}_0^T D_{he} + D_{ee}) \bar{\epsilon} \equiv \frac{1}{2} \bar{\epsilon}^T \bar{D} \bar{\epsilon} \quad (30)$$

Clearly \bar{D} is the so-called effective (or homogenized) material matrix and $\bar{\epsilon}$ the global strains. The effective medium has an energy density Π_Ω , which can be used to carry out macroscopic analyses.

If the local fields within the UC are of interest, we can recover those fields based on the global displacements v , global strains $\bar{\epsilon}$, and the fluctuation functions χ . To this end, we need to uniquely determine the fluctuation functions first, otherwise, we could not uniquely determine the local displacement field. Recall, we fixed an arbitrary node and made nodes on the positive boundary surfaces slave to facilitate the solution for the fluctuation functions. First, we need to construct a new array $\tilde{\mathcal{X}}_0$ from \mathcal{X}_0 by assigning the values for slave nodes according to the corresponding active nodes and assign zeros to the fixed node. Obviously, $\tilde{\mathcal{X}}_0$ still yields the minimum value of Π_Ω in Eq. (22) under constraints in Eqs. (15)–(17). However, $\tilde{\mathcal{X}}_0$ may not satisfy the constraints in Eq. (21) because it is different from the real solution by a constant. To find the real solution, denoting as $\bar{\mathcal{X}}_0$, we need to construct a discretized version of Eq. (21). Let us rewrite Eq. (21) as

$$\int_\Omega \chi^T \psi d\Omega = 0 \quad (31)$$

with ψ as the 3×3 identity matrix. It can be easily verified that ψ is the kernel matrix of Γ_h in Eq. (24). Both χ and ψ can discretized using the finite elements as

$$\chi = \bar{S} \bar{\mathcal{X}} \quad \psi = \bar{S} \Psi \quad (32)$$

with Ψ as the discretized kernel matrix. Substituting Eq. (32) to Eq. (31), we can obtain the discretized version of the constraints as:

$$\bar{\mathcal{X}}^T H \Psi = 0 \quad (33)$$

with $H = \int_{\Omega} \bar{S}^T S d\Omega$. Please note that we can always normalize the kernel matrix so that $\Psi^T H \Psi = \psi$.

The real solution $\bar{\mathcal{X}}$ can be expressed as

$$\bar{\mathcal{X}} = \tilde{\mathcal{X}}_0 \bar{\epsilon} + \Psi \lambda \quad (34)$$

where λ are constants to be determined. Substituting the above relation into Eq. (33), we can solve λ as

$$\lambda = -\Psi^T H \tilde{\mathcal{X}}_0 \bar{\epsilon} \quad (35)$$

Then, the real solution is

$$\bar{\mathcal{X}} = (I - \Psi \Psi^T H) \tilde{\mathcal{X}}_0 \bar{\epsilon} \equiv \bar{\mathcal{X}}_0 \bar{\epsilon} \quad (36)$$

with I as the $n \times n$ identity matrix and n is the total number of degrees of freedom.

After the fluctuation functions are determined uniquely, we can recover the local displacement based on Eqs. (9), (12), and (32) as

$$u = v + \begin{bmatrix} \frac{\partial v_1}{\partial x_1} & \frac{\partial v_1}{\partial x_2} & \frac{\partial v_1}{\partial x_3} \\ \frac{\partial v_2}{\partial x_1} & \frac{\partial v_2}{\partial x_2} & \frac{\partial v_2}{\partial x_3} \\ \frac{\partial v_3}{\partial x_1} & \frac{\partial v_3}{\partial x_2} & \frac{\partial v_3}{\partial x_3} \end{bmatrix} \begin{Bmatrix} y_1 \\ y_2 \\ y_3 \end{Bmatrix} + \bar{S} \bar{\mathcal{X}}_0 \bar{\epsilon} \quad (37)$$

with u as the column matrix of u_i and v as the column matrix of v_i . The local strain field can be recovered using Eqs. (6) and (24) as

$$\epsilon = \bar{\epsilon} + \Gamma_h \bar{S} \bar{\mathcal{X}}_0 \bar{\epsilon} \quad (38)$$

Finally, the local stress field can be recovered straightforwardly as

$$\sigma = D \epsilon \quad (39)$$

It can be easily verified that

$$\langle \sigma \rangle = \bar{D} \bar{\epsilon} \quad (40)$$

which is expected because the effective material matrix can be equivalently defined through the energy density of the UC or the relation between the average stress and average strain of the UC. In comparison to common numerical micromechanical simulations in the literature, the present implementation is unique in the following aspects:

- No external load is necessary to perform the simulation and the complete set of material properties can be predicted within one analysis.
- The fluctuation functions and local displacements can be determined uniquely;
- The effective material properties and recovered local fields are calculated directly with the same accuracy of the fluctuation functions. No postprocessing type calculations which introduces more approximations are needed.

- The dimensionality of the problem is determined by that of the periodicity of the UC. A complete set of 3D material properties can be obtained using a 1D analysis of microstructures with 1D periodicity such as binary composites. It is noted that the macroscopic analysis of a structure made with material having 1D periodicity could be 3D, which requires the complete set of effective material properties.

We have coded the above formulation using Fortran 90/95 into a program named VAMUCH. To demonstrate the application, accuracy, and efficiency of this theory and code, we will analyze several material systems using VAMUCH in the next section.

5. Validation of VAMUCH

VAMUCH provides a unified analysis for general 1D, 2D, or 3D UCs. First, the same code VAMUCH can be used to homogenize binary composites (modeled using 1D UCs), fiber reinforced composites (modeled using 2D UCs), and particle reinforced composites (modeled using 3D UCs). Second, VAMUCH can reproduce the results for lower-dimensional UCs using higher-dimensional UCs. That is, VAMUCH will predict the same results for binary composites using 1D, 2D or 3D UCs, and for fiber reinforced composites using 2D or 3D UCs.

5.1. Binary composites

First, let us consider a periodic binary composite formed by orthotropic layers and the material axes are the same as the global coordinates x_i so that the material is uniform in the $x_1 - x_2$ plane and periodic along x_3 direction. A typical UC can be identified as shown in Fig. 4, the dimension along y_3 is h and dimensions along y_1 and y_2 can be arbitrary. Let ϕ_1 and ϕ_2 denote the volume fractions of the first phase and the second phase, respectively, and we have $\phi_1 + \phi_2 = 1$. This problem has been solved analytically in Yu (2005). The strain energy density of the effective material can be obtained as:

$$\Pi_{\Omega} = \frac{1}{2} \begin{Bmatrix} \bar{\epsilon}_{11} \\ 2\bar{\epsilon}_{12} \\ \bar{\epsilon}_{22} \\ 2\bar{\epsilon}_{13} \\ 2\bar{\epsilon}_{23} \\ \bar{\epsilon}_{33} \end{Bmatrix}^T \begin{bmatrix} c_{11}^* & 0 & c_{13}^* & 0 & 0 & c_{16}^* \\ 0 & c_{22}^* & 0 & 0 & 0 & 0 \\ c_{13}^* & 0 & c_{33}^* & 0 & 0 & c_{36}^* \\ 0 & 0 & 0 & c_{44}^* & 0 & 0 \\ 0 & 0 & 0 & 0 & c_{55}^* & 0 \\ c_{16}^* & 0 & c_{36}^* & 0 & 0 & c_{66}^* \end{bmatrix} \begin{Bmatrix} \bar{\epsilon}_{11} \\ 2\bar{\epsilon}_{12} \\ \bar{\epsilon}_{22} \\ 2\bar{\epsilon}_{13} \\ 2\bar{\epsilon}_{23} \\ \bar{\epsilon}_{33} \end{Bmatrix} \quad (41)$$

It can be observed that the homogenized material properties still have the same orthotropic symmetry for this special case, although in general the homogenized material could be anisotropic, which means a fully populated 6×6 stiffness matrix. The expressions of effective material properties c_{ij}^* are listed here.

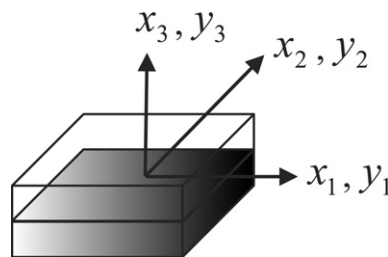


Fig. 4. Sketch of a binary composite.

$$\begin{aligned}
c_{11}^* &= \langle c_{11} \rangle - \frac{\phi_1 \phi_2 (c_{16}^{(2)} - c_{16}^{(1)})^2}{\phi_1 c_{66}^{(2)} + \phi_2 c_{66}^{(1)}} \\
c_{13}^* &= \langle c_{13} \rangle - \frac{\phi_1 \phi_2 (c_{16}^{(2)} - c_{16}^{(1)}) (c_{36}^{(2)} - c_{36}^{(1)})}{\phi_1 c_{66}^{(2)} + \phi_2 c_{66}^{(1)}} \\
c_{16}^* &= \frac{\phi_1 c_{16}^{(1)} c_{66}^{(2)} + \phi_2 c_{16}^{(2)} c_{66}^{(1)}}{\phi_1 c_{66}^{(2)} + \phi_2 c_{66}^{(1)}} \\
c_{33}^* &= \langle c_{33} \rangle - \frac{\phi_1 \phi_2 (c_{36}^{(2)} - c_{36}^{(1)})^2}{\phi_1 c_{66}^{(2)} + \phi_2 c_{66}^{(1)}} \\
c_{36}^* &= \frac{\phi_1 c_{36}^{(1)} c_{66}^{(2)} + \phi_2 c_{36}^{(2)} c_{66}^{(1)}}{\phi_1 c_{66}^{(2)} + \phi_2 c_{66}^{(1)}} \\
c_{66}^* &= 1 / \left\langle \frac{1}{c_{66}} \right\rangle \quad c_{55}^* = 1 / \left\langle \frac{1}{c_{55}} \right\rangle \quad c_{44}^* = 1 / \left\langle \frac{1}{c_{44}} \right\rangle \quad c_{22}^* = \langle c_{22} \rangle
\end{aligned} \tag{42}$$

where the superscripted quantities are those from each phase of the composite. It can be observed that even for this simple case, only c_{22}^* is the same as the rule of mixture based on the Voigt hypothesis, and $c_{44}^*, c_{55}^*, c_{66}^*$ are the same as the rule of mixture based on the Reuss hypothesis. All the other components are different from these two rules of mixture. The effective material properties of the present theory reproduce those of a mathematical homogenization theory in [Manevitch et al. \(2002\)](#). When both layers are made of isotropic material, having Lamé properties λ_1, μ_1 for layer 1 and λ_2, μ_2 for layer 2, the formulas in Eq. (42) reproduce the well-known exact expressions listed on Page 140 of [Christensen \(1979\)](#) which was obtained by [Postma \(1955\)](#).

[Yu \(2005\)](#) shows that the fluctuation functions are piecewise linear functions for binary composites, which means we can use 2-noded line elements for 1D UC in VAMUCH to exactly, in the numerical sense, reproduce the analytical solution. We have also obtained the same results using 2D and 3D UCs numerically. For the sake of saving space, such results are not presented here. Suffice to state that the numerical results from VAMUCH are exactly the same as the analytical solution within the machine precision.

5.2. Fiber reinforced composites

To show the predictive capability of VAMUCH for unidirectional fiber reinforced composites, we choose a few examples extensively studied in the literature. For the first two examples, comparisons are made between FEM ([Sun and Vaidya, 1996](#)), method of cell (MOC) ([Aboudi, 1982](#)), generalized method of cell (GMC) ([Paley and Aboudi, 1992](#)), high-fidelity generalized method of cell (HFGMC) ([Aboudi et al., 2001](#)), and elasticity-based cell method (ECM) ([Williams, 2005b](#)). The FEM approach of [Sun and Vaidya \(1996\)](#) is established on a rigorous mechanics foundation and 3D RVEs with periodic boundary conditions are used for homogenization. The MOC and its variants (GMC, HFGMC, and ECM) expand the local displacements in terms of global displacements using the Legendre polynomials of different orders. ECM starts from this assumption and solve the equations of continuum mechanics in a strong form. In contrast, MOC, GMC, and HFGMC invokes additional *ad hoc* assumptions such as that the interfacial continuous conditions and periodic boundary conditions are only satisfied in the integral sense. FEM results are directly taken from [Sun and Vaidya \(1996\)](#), MOC and ECM results from [Williams \(2005b\)](#), GMC and HFGMC results from [Aboudi et al. \(2001\)](#).

The first example is a boron/aluminum composite. Both constituents are isotropic with Young's modulus $E = 379.3$ GPa and Poisson's ratio $\nu = 0.1$ for boron fibers, and $E = 68.3$ GPa and $\nu = 0.3$ for aluminum matrix. The fiber is of circular shape and arranged in a square array (see the sketch in the middle of [Fig. 1](#)) and the fiber volume fraction is 0.47. The effective material properties predicted by different approaches are listed in [Table 1](#). It can be observed that MOC and GMC significantly underpredict the shear moduli G_{12}

Table 1
Effective material properties of boron/aluminum composites

| Models | E_{11} (GPa) | E_{22} (GPa) | G_{12} (GPa) | G_{23} (GPa) | ν_{12} | ν_{23} |
|--------|----------------|----------------|----------------|----------------|------------|------------|
| VAMUCH | 215.3 | 144.1 | 54.39 | 45.92 | 0.195 | 0.255 |
| FEM | 215 | 144 | 57.2 | 45.9 | 0.19 | 0.29 |
| MOC | 215 | 142.6 | 51.3 | 43.7 | 0.20 | 0.25 |
| GMC | 215.0 | 141.0 | 51.20 | 43.70 | 0.197 | 0.261 |
| HFGMC | 215.4 | 144.0 | 54.34 | 45.83 | 0.195 | 0.255 |
| ECM | 215 | 143.4 | 54.3 | 45.1 | 0.19 | 0.26 |

Table 2
Effective material properties of graphite/epoxy composites

| Models | E_{11} (GPa) | E_{22} (GPa) | G_{12} (GPa) | G_{23} (GPa) | ν_{12} | ν_{23} |
|--------|----------------|----------------|----------------|----------------|------------|------------|
| VAMUCH | 142.9 | 9.61 | 6.10 | 3.12 | 0.252 | 0.350 |
| FEM | 142.6 | 9.60 | 6.00 | 3.10 | 0.25 | 0.35 |
| MOC | 143 | 9.6 | 5.47 | 3.08 | 0.25 | 0.35 |
| GMC | 143.0 | 9.47 | 5.68 | 3.03 | 0.253 | 0.358 |
| HFGMC | 142.9 | 9.61 | 6.09 | 3.10 | 0.252 | 0.350 |
| ECM | 143 | 9.6 | 5.85 | 3.07 | 0.25 | 0.35 |

and G_{23} while FEM overpredicts the longitudinal shear modulus G_{12} . The closest correlation for all the values is found between VAMUCH and HFGMC.

The second example is graphite/epoxy composites. Graphite fiber is transversely isotropic with $E_{11} = 235$ GPa, $E_{22} = 14$ GPa, $G_{12} = 28$ GPa, $\nu_{12} = 0.2$, and $\nu_{23} = 0.25$. Epoxy matrix is isotropic with $E = 4.8$ GPa and $\nu = 0.34$. The fiber is circular and arranged in a square array and the fiber volume fraction is 0.6. The results from different approaches are listed in Table 2. Again the closest correlation is found between VAMUCH and HFGMC. Considering the fact that HFGMC uses the governing equations of MHT and that VAMUCH can reproduce MHT, it is not surprising to find out that HFGMC has an excellent agreement with VAMUCH. The FEM and ECM predictions are also very close to VAMUCH results for this case. It is noted that the ECM results listed in Tables 1 and 2 are obtained from the 3rd order model. If the 5th order theory is used, the correlation between ECM and VAMUCH might be improved as shown in the following two examples.

In the following two examples, VAMUCH is compared with MOC, ECM (both 3rd order and 5th order), Green's function based approach (G-F) (Walker et al., 1993) and FEM. The results of MOC, ECM, and G-F are directly taken from Williams (2005b), while FEM results are calculated using ANSYS following the approach proposed in Sun and Vaidya (1996). To be consistent with Williams (2005b), we use 2D UCs having square inclusions in the center for VAMUCH. As pointed out in Williams (2005b), square inclusions provide a stringent test of correct modeling the local and global behavior of heterogeneous materials due to strong gradients in the local fields induced by the corners. The two material systems we consider are tungsten/copper composite and void/copper composite. Both tungsten and copper are assumed to be isotropic with $E = 395.0$ GPa and $\nu = 0.28$ for tungsten, and $E = 127.0$ GPa and $\nu = 0.34$ for copper.

For both material systems, we calculate the effective transverse Young's modulus at different inclusion volume fractions of 0.0204, 0.1837, 0.5102, and 0.7511. The results are listed in Table 3 for tungsten/copper composite and Table 4 for void/copper composite. It is verified that the FEM approach of Sun and Vaidya has no size effects for E_{22} , which means this approach will provide the most accurate prediction of E_{22} with a converged mesh. As one can observe from Tables 3 and 4, MOC and 3rd order ECM underpredict this value up to 1.6% for tungsten/copper composite and 8.6% for void/copper composite. VAMUCH, G-F, and 5th order ECM have excellent agreement with FEM, with VAMUCH having the closest correlations.

To show the effect of shape of inclusions, we predict the effective transverse Young's modulus using UC with circular inclusions arranged in a square array. As shown in Tables 3 and 4, the shape effects of inclusions become more and more significant and cannot be neglected with large volume fraction of inclusions, partic-

Table 3

 E_{22} (GPa) of W/Cu composites varying with fiber volume fraction

| Models | 0.0204 | 0.1837 | 0.5102 | 0.7511 |
|-------------------|--------|--------|--------|--------|
| VAMUCH | 129.92 | 156.51 | 229.72 | 300.99 |
| FEM | 129.92 | 156.51 | 229.71 | 301.0 |
| G-F | 129.87 | 156.18 | 229.09 | 300.70 |
| MOC | 129.50 | 154.40 | 226.20 | 299.00 |
| ECM (3rd order) | 129.50 | 154.60 | 226.60 | 299.10 |
| ECM (5th order) | 129.80 | 156.50 | 229.50 | 300.80 |
| VAMUCH (circular) | 129.81 | 155.19 | 226.94 | 298.12 |
| FEM (circular) | 129.82 | 155.20 | 226.97 | 298.14 |

Table 4

 E_{22} (GPa) of Void/Cu composites varying with void volume fraction

| Models | 0.0204 | 0.1837 | 0.5102 | 0.7511 |
|-------------------|--------|--------|--------|--------|
| VAMUCH | 120.22 | 81.73 | 39.75 | 18.25 |
| FEM | 120.22 | 81.70 | 39.75 | 18.25 |
| G-F | 120.63 | 83.50 | 40.48 | 18.40 |
| MOC | 110.20 | 75.27 | 38.22 | 17.99 |
| ECM (3rd) | 110.20 | 75.38 | 38.23 | 17.99 |
| ECM (5th) | 118.90 | 80.97 | 39.64 | 18.20 |
| VAMUCH (circular) | 120.34 | 82.67 | 39.08 | 10.31 |
| FEM (circular) | 120.34 | 82.64 | 39.08 | 10.31 |

ularly for void/copper composites. For example, E_{22} of void/copper composite with square holes is 80% larger than the composite with circular holes, when the void volume fraction reaches 0.7511. It is interesting to note that E_{22} of the W/Cu composite with square inclusions is slightly larger than that with circular inclusions, with the difference getting bigger with larger fiber volume fraction. However, for the case of Void/Cu, material with square voids is slightly smaller than that with circular voids for small void volume fractions. As the void volume fraction getting bigger the trend is reversed. A parametric study is carried out to find out the point where

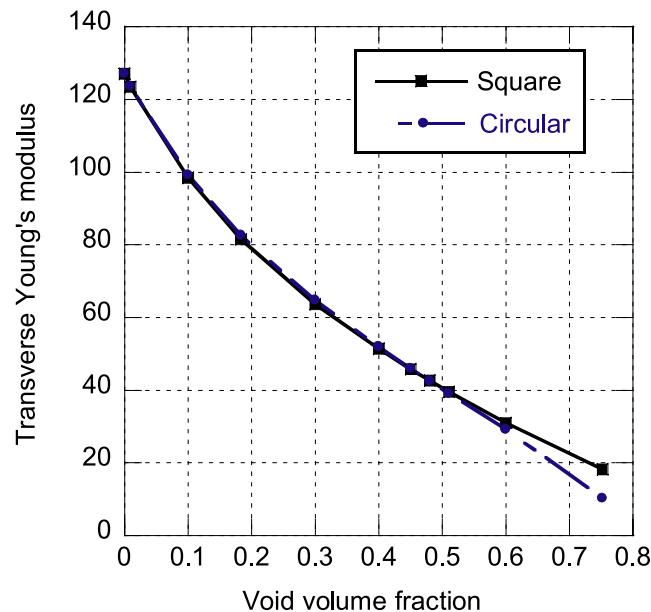


Fig. 5. Change of Young's modulus of material with square voids and circular voids with respect to void volume fractions.

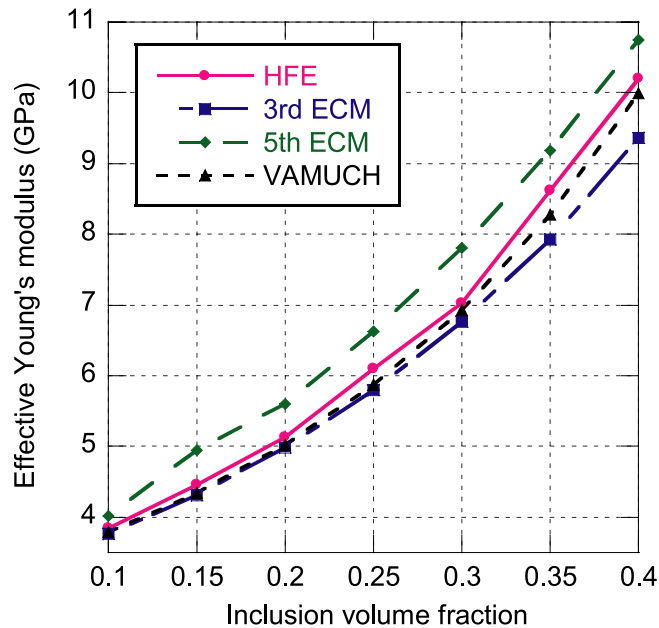


Fig. 6. Effective Young's modulus of glass/epoxy composite with spherical inclusions.

the trend is reversed. As observed from Fig. 5, when the void volume fraction is greater than zero and less than 0.45 (approximate), E_{22} of materials having square voids are slightly smaller than those having circular voids. When the void volume fraction is greater than 0.45 (approximate), materials with square voids have bigger E_{22} than those with circular voids.

5.3. Particle reinforced composites

Due to special arrangements of constituents of particle reinforced composites, 3D UCs are required to accurately model the microstructures. We are going to use VAMUCH to analyze several particle reinforced composites to validate its 3D capability. In previous section, we have shown that the prediction of MOC and GMC is not accurate for fiber reinforced composites and one could infer that they can not provide very accurate prediction for particle reinforced composites either. Although HFGMC and G-F provide excellent prediction for fiber reinforced composites, we could not find 3D examples analyzed by these two approaches. It is easy to verify that Sun and Vaidya's FEM approach is equally applicable to particle reinforced composites. Two other approaches we believe will provide critical evaluations for VAMUCH are the 3D version of ECM (Williams, 2005a) and an approach based on mathematical homogenization theory and finite element method (Banks-Sills et al., 1997) (later we follow Williams (2005a) to name this approach as HFE).

The first example is to predict the effective Young's modulus for a glass/epoxy composite. The UC of this composite is composed of glass spheres embedded in a triply periodic cubic array. Both constituents are isotropic with Young's modulus $E = 76.00$ GPa and Poisson's ratio $\nu = 0.23$ for glass, and Young's modulus $E = 3.01$ GPa and Poisson's ratio $\nu = 0.394$ for epoxy.² We plot the change of effective Young's modulus with respect to the inclusion volume fraction in Fig. 6. In comparison to HFE, VAMUCH outperforms ECM (both 3rd order and 5th order). We are surprised to find out that it is counter intuitive that the predictions of 5th order ECM are worse than 3rd order ECM for this particular case. It is worthy to point out that the data of HFE and ECM are provided independently by the author of Williams (2005a), where ECM data are calculated and HFE data are directly picked out from the plots in Banks-Sills et al. (1997).

² The isotropic assumption is convenient for comparing with available results in the literature. VAMUCH can deal with constituents with full anisotropy with material properties characterized as many as 21 independent constants.

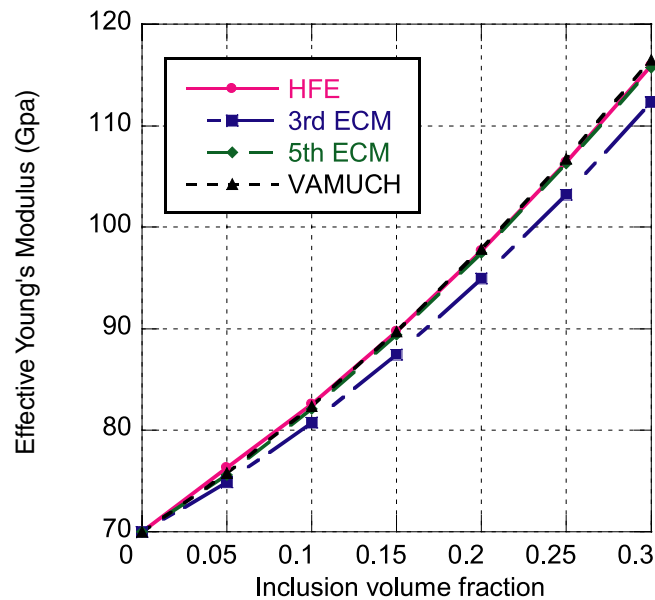


Fig. 7. Effective Young's modulus of $\text{Al}_2\text{O}_3/\text{Al}$ composites with cubic inclusions.

The second example is a $\text{Al}_2\text{O}_3/\text{Al}$ composite with cubic inclusions in a cubic array. Both constituents are isotropic with Young's $E = 350.00$ GPa and Poisson's ratio $\nu = 0.30$ for aluminum oxide, and Young's modulus $E = 70.00$ GPa and Poisson's ratio $\nu = 0.30$ for aluminum. The effective Young's modulus and Poisson's ratio are plotted in Figs. 7 and 8, respectively. It can be observed that both VAMUCH and 5th order ECM have an excellent agreement with HFE while the predictions of 3rd order ECM are not as accurate.

The last example is a $\text{Al}_2\text{O}_3/\text{Al}$ composite having rectangular parallelepiped inclusions with the ratio between the three dimensions as $a_1/a_2/a_3 = 2/1/2$ where a_i is the dimension of the inclusion along the corre-

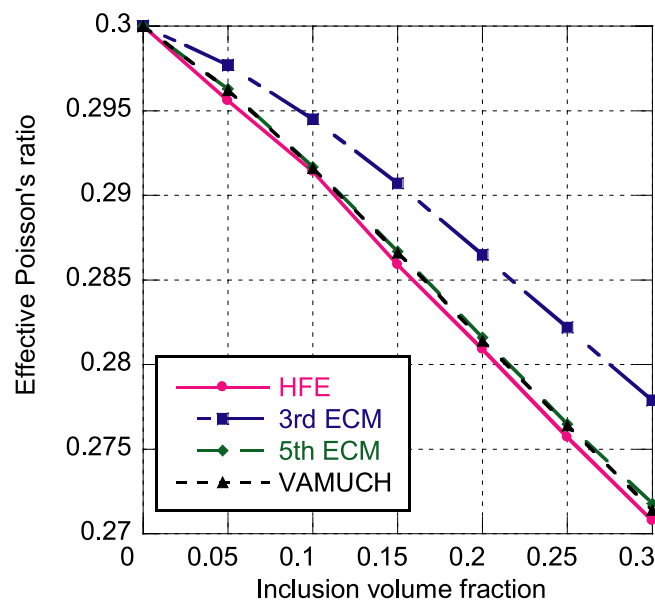


Fig. 8. Effective Poisson's ratio of $\text{Al}_2\text{O}_3/\text{Al}$ composites with cubic inclusions.

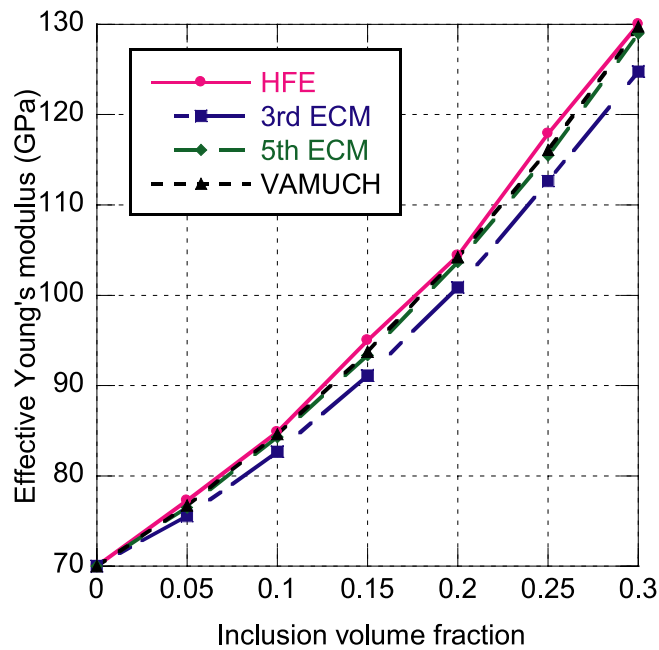


Fig. 9. Effective Young's modulus E_{33} of $\text{Al}_2\text{O}_3/\text{Al}$ composites with rectangular parallelepiped inclusions.

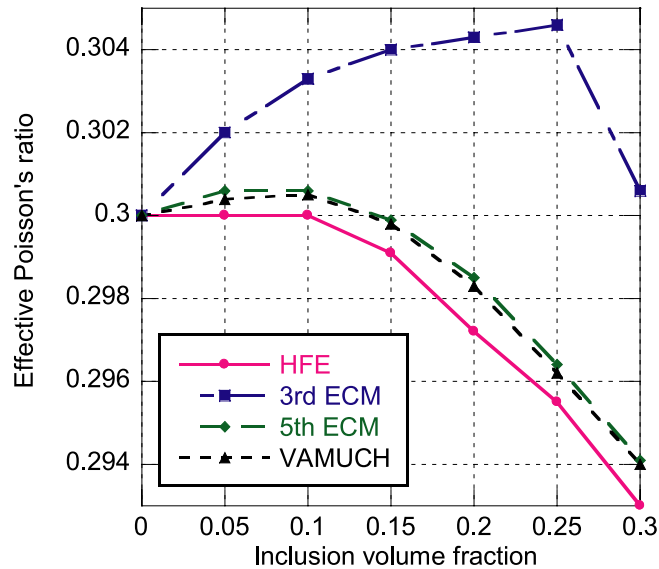


Fig. 10. Effective Poisson's ratio ν_{12} of $\text{Al}_2\text{O}_3/\text{Al}$ composites with rectangular parallelepiped inclusions.

sponding y_i direction. The effective material properties of this composite is not isotropic any more. For the sake of saving space, we only plot the effective Young's modulus E_{33} and effective Poisson's ratio ν_{12} as functions of inclusion volume fraction in Figs. 9 and 10, respectively. Again VAMUCH and 5th order ECM have excellent agreements with HFE and outperform 3rd order ECM.

6. Conclusion

A new micromechanics model, the variational asymptotic method for unit cell homogenization (VAMUCH), has been developed to homogenize heterogeneous materials and recover the local fields within the microstructure after obtaining the global responses of the material. VAMUCH provides a uniform analysis for microstructures which can be described using 1D, 2D, or 3D UCs, such as binary composites, fiber-reinforced composites, and particle-reinforced composites. In comparison to existing micromechanics approaches, VAMUCH has the following major advantages:

- (1) VAMUCH adopts the variational asymptotic method as its mathematical foundation. It has the same rigor as MHT without even assuming periodic fluctuation functions and boundary conditions. VAMUCH uses only assumptions inherent in micromechanics without invoking any additional *ad hoc* assumptions.
- (2) VAMUCH has an inherent variational nature and its numerical implementation is shown to be straightforward.
- (3) VAMUCH handles 1D/2D/3D unit cells uniformly. The dimensionality of the problem is determined by that of the periodicity of the unit cell.
- (4) VAMUCH can obtain different material properties in different directions simultaneously, which is more efficient than those approaches requiring multiple runs under different loading conditions.
- (5) VAMUCH calculates effective properties and local fields directly with the same accuracy as the fluctuation functions. No postprocessing calculations such as stress averaging and strain averaging are needed.

The companion code, VAMUCH, is extensively validated using various examples including binary composites, fiber reinforced composites, and particle reinforced composites. We can confidently conclude that VAMUCH provides a versatile and convenient tool for engineers to efficiently yet accurately design and analyze heterogeneous materials.

Acknowledgements

This study was supported by NSF under Grant DMI-0522908. The views and findings contained herein are those of the authors and should not be interpreted as necessarily representing the official policies or endorsement, either expressed or implied, of NSF. The authors want to thank Dr. Todd O. Williams from Los Alamos National Laboratory for technical discussions and providing the data of ECM and HFE for particle reinforced composites. The authors also want to thank Dr. Victor Berdichevsky of Wayne State University, the author of Variational Asymptotic Method, for technical discussions and advise.

References

- Aboudi, J., 1982. A continuum theory for fiber-reinforced elastic-visoplastic composites. *International Journal of Engineering Science* 20 (5), 605–621.
- Aboudi, J., 1989. Micromechanical analysis of composites by the method of cells. *Applied Mechanics Reviews* 42 (7), 193–221.
- Aboudi, J., Pindera, M.J., Arnold, S.M., 2001. Linear thermoelastic higher-order theory for periodic multiphase materials. *Journal of Applied Mechanics* 68, 697–707.
- Accorsi, M.L., Nemat-Nasser, S., 1986. Bounds on the overall elastic and instantaneous elastoplastic moduli of periodic composites. *Mechanics of Materials* 5 (3), 209–220.
- Banerjee, B., Adams, D.O., 2004. On predicting the effective elastic properties of polymer bonded explosives using the recursive cell method. *International Journal of Solids and Structures* 41 (2), 481–509.
- Banks-Sills, L., Leiderman, V., Fang, D., 1997. On the effect of particle shape and orientation on elastic properties of metal matrix composites. *Composites Part B: Engineering* 28B, 465–481.
- Bensoussan, A., Lions, J., Papanicolaou, G., 1978. *Asymptotic Analysis for Periodic Structures*. North-Holland, Amsterdam.
- Berdichevsky, V.L., 1977. On averaging of periodic systems. *PMM* 41 (6), 993–1006.
- Berdichevsky, V.L., 1979. Variational-asymptotic method of constructing a theory of shells. *PMM* 43 (4), 664–687.
- Christensen, R.M., 1979. *Mechanics of Composite Materials*. Wiley-Interscience, New York.
- Dvorak, G.J., Bahei-El-Din, Y.A., 1979. Elastic-plastic behavior of fibrous composites. *Journal of Mechanics and Physics of Solids* 27, 51–72.
- Guedes, J.M., Kikuchi, N., 1990. Preprocessing and postprocessing for materials based on the homogenization method with adaptive finite element method. *Computer Methods in Applied Mechanics and Engineering* 83, 143–198.

- Hashin, Z., 1983. Analysis of composite materials-a survey. *Applied Mechanics Review* 50, 481–505.
- Hashin, Z., Shtrikman, S., 1962. A variational approach to the theory of the elastic behaviour of polycrystals. *Journal of Mechanics and Physics of Solids* 10, 343–352.
- Hill, R., 1952. The elastic behavior of crystalline aggregate. *Proceedings of the Physical Society of London A* 65, 349–354.
- Hill, R., 1965. Theory of mechanical properties of fibre-strengthened materials-iii. Self-consistent model. *Journal of Mechanics and Physics of Solids* 13, 189–198.
- Hollister, S.J., Kikuchi, N., 1992. A comparison of homogenization and standard mechanics analyses for periodic porous composites. *Computational Mechanics*.
- Kunin, I., 1982 *Theory of Elastic Media with Microstructure*, Vol. 1 and 2. Springer Verlag, Berlin.
- Manevitch, L.I., Andrianov, I.V., Oshmyan, V.G., 2002. *Mechanics of Periodically Heterogeneous Structures*. Springer, Berlin.
- Milton, G.W., 1981. Bounds on the electromagnetic, elastic and other properties of two component composites. *Physics Review Letters* 46 (8), 542–545.
- Murakami, H., Toledano, A., 1990. A higher-order mixture homogenization of bi-laminated composites. *Journal of Applied Mechanics* 57, 388–396.
- Paley, M., Aboudi, J., 1992. Micromechanical analysis of composites by the generalized cells model. *Mechanics of Materials* 14, 127–139.
- Postma, G.W., 1955. Wave propagation in a stratified medium. *Geophysics* 20, 780.
- Sun, C.T., Vaidya, R.S., 1996. Prediction of composite properties from a representative volume element. *Composites Science and Technology* 56, 171–179.
- Walker, K.P., Freed, A.D., Jordan, E.H., 1993. Accuracy of the generalized self-consistent method in modeling the elastic behavior of periodic composite properties of unidirectional fiber-reinforced composites and their sensitivity coefficients. *Philosophical Transactions of the Royal Society of London A* 345, 545–576.
- Williams, T.O., 2005a. A three-dimensional, higher-order, elasticity-based micromechanics model. *International Journal of Solids and Structures* 42, 971–1007.
- Williams, T.O., 2005b. A two-dimensional, higher-order, elasticity-based micromechanics model. *International Journal of Solids and Structures* 42, 1009–1038.
- Yu, W., 2005. A variational-asymptotic cell method for periodically heterogeneous materials. In: *Proceedings of the 2005 ASME International Mechanical Engineering Congress and Exposition*. ASME, Orlando, Florida.
- Yu, W., Hodges, D.H., 2004a. An asymptotic approach for thermoelastic analysis of laminated composite plates. *Journal of Engineering Mechanics* 130 (5), 531–540.
- Yu, W., Hodges, D.H., 2004b. A simple thermopiezoelectric model for composite plates with accurate stress recovery. *Smart Materials and Structures* 13 (4), 926–938.
- Yu, W., Hodges, D.H., 2005. Mathematical construction of an engineering thermopiezoelectric model for smart composite shells. *Smart Materials and Structures* 14 (1), 43–55.
- Yu, W., Hodges, D.H., Volovoi, V.V., 2002a. Asymptotic construction of Reissner-like models for composite plates with accurate strain recovery. *International Journal of Solids and Structures* 39 (20), 5185–5203.
- Yu, W., Hodges, D.H., Volovoi, V.V., 2002b. Asymptotic generalization of Reissner-Mindlin theory: accurate three-dimensional recovery for composite shells. *Computer Methods in Applied Mechanics and Engineering* 191 (44), 5087–5109.
- Yu, W., Hodges, D.H., Volovoi, V.V., Cesnik, C.E.S., 2002c. On Timoshenko-like modeling of initially curved and twisted composite beams. *International Journal of Solids and Structures* 39 (19), 5101–5121.